Chapter 4
From Spectator Species to Active Site Using X-ray Absorption and Emission Spectroscopy Under Realistic Conditions

Maarten Nachtegaal, Urs Hartfelder and Jeroen A. van Bokhoven

Abstract X-ray absorption and emission spectroscopy experiments on metal-supported catalysts are described. Time- and space-resolved spectroscopy measurements enable determining the electronic and geometric structures of the catalytically active elements at any location within a real reactor and under actual reaction conditions. Methods that distinguish spectator from active species are described. The data survey shows that there is not one single phase that is responsible for activity. Conversion leads to changes in gas composition, affecting the structure. Within a single reactor, multiple phases can be present, which is certainly the case under oscillating conditions. Platinum catalysts contain lowly-active phases that are associated with carbon monoxide poisoning. Highly-active phases form after complete desorption of carbon monoxide. Such a surface is also prone to very rapid surface oxidation. The relationship between these phases and catalytic activity in carbon monoxide oxidation is discussed.

4.1 Introduction

In situ and *operando* catalyst characterization methods using X-ray absorption and emission spectroscopy (XAS and XES) are indispensable tools to determine the structure of catalytically-active sites under working conditions [1, 2]. By using these techniques, the local electronic and geometric structure (up to ca. 6 Å) around

M. Nachtegaal
Paul Scherrer Institute, 5236 Villigen, Switzerland
e-mail: maarten.nachtegaal@psi.ch

U. Hartfelder · J.A. van Bokhoven (✉)
Institute for Chemical and Bioengineering, ETH Zurich, 8093 Zurich, Switzerland
e-mail: jeroen.vanbokhoven@chem.ethz.ch

U. Hartfelder
e-mail: urs.hartfelder@chem.ethz.ch

J.A. van Bokhoven
Paul Scherrer Institute, 5236 Villigen, Switzerland

the atom of interest can be determined. X-rays of sufficiently high energy (4 keV or higher) have a high penetration depth, so that catalysts in an actual reactor can be measured and the catalyst structure under reaction conditions can be accessed in an element-specific manner. Because of the strong interaction of reactants and intermediates with the catalyst surface, the catalyst structure varies with the conditions. To perform time-resolved XAS or XES experiments, a high flux of X-rays is needed, which is provided by synchrotron light sources. In general, each synchrotron has at least one beam line dedicated to X-ray spectroscopy, many of which are dedicated to catalysis research [3].

In an X-ray absorption experiment, a monochromatic X-ray beam is scanned around the absorption edge of the element of interest. A core electron is excited by a photon when the energy of the incoming photon matches or exceeds the binding energy of that core electron. At that energy, a sudden jump in absorption occurs (Fig. 4.1). The exceeding energy of the incoming photon is given to the outgoing photon as kinetic energy. Because the absorption coefficient is a function of the X-ray energy, the absorption signal is modulated. Just above the absorption edge, the outgoing photon does not contain enough kinetic energy to be excited into the vacuum and instead could be excited to unoccupied electronic states. In case of excitation of an electron in the K shell, a 1s electron is excited into empty p density of states, which is the dipolar transition, respectively empty d density of states, the quadrupolar transition. Exciting an electron from the L shell probes p density of states (L_1 edge, 2s electron excitation), respectively d density of states ($L_{2,3}$ edges, 2p excitation). From these considerations, the following becomes clear: i. XAS is element specific, because of the unique binding energy of each element's electron; ii. X-ray absorption K and L_1 edge spectra measure the empty p density of states and are thus sensitive to geometry and oxidation state; iii. $L_{2,3}$ edge spectra probe empty d density of states. In case of K edge absorption, the weak signals of the
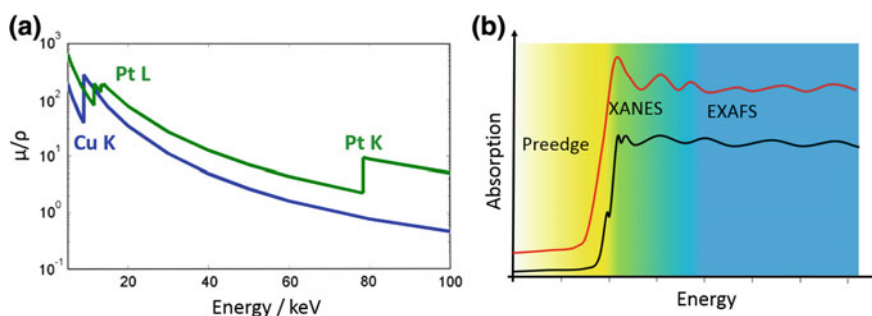

Fig. 4.1 Transmission of X-rays through matter as function of X-ray energy. Sharp rises in absorption occur at energies equal to the binding energy of electrons (**a**). A XAS spectrum is typically divided into three regions, the *pre-edge*, the *XANES*, and the *EXAFS* regions (**b**). The *pre-edge* and *XANES* are separated by the absorption edge, characterized by the sharp increase in X-ray absorption. The *bottom line* corresponds to a Cu K-edge spectrum, the *top line* to a Pt L_3-edge XAS spectrum

quadrupolar transition probe d density of states. When measuring transition metals, measuring the L_3 edge may be attractive, because it tracks the anti-bonding states of adsorbates on the surface and is sensitive to the mode of adsorption in a quantitative manner (Fig. 4.2) [4]. In summary, the X-ray absorption near edge region (XANES) provides element-specific information on the empty density of states.

Observing the modulation of absorption over a much longer energy interval yields EXAFS data, which probe the local environment around the X-ray absorbing atom. The averaged coordination, the distance to the near neighbors, and the disorder (Debye-Waller factor) can be obtained from fitting of the EXAFS spectra [5].

In addition to X-ray absorption, X-ray emission yields complementary information. An X-ray emission spectrum tracks the emitted fluorescence upon elimination of the core-hole generated by the photon absorption. This experiment probes the filled density of states and is thus a complimentary tool to determine the electronic structure. Because the type of neighbors and oxidation state determine the electronic structure X-ray emission spectroscopy is a sensitive tool for their determination [6–8].

In situ cells that enable measuring X-ray absorption and X-ray emission spectroscopy on working catalysts have been around for many decades [9]. They can be constructed because the X-rays of sufficiently high energy used for X-ray absorption and emission spectroscopy penetrate through thin reactor walls. Heterogeneous and homogeneous reactions can be accessed at high pressure (in excess of 100 s bar) and temperature (beyond 1000 °C) [10]. Such measurements yield the structure of the functioning catalyst, sometimes performed under industrial conditions. A complication of the high penetration depth of X-rays is that an average of all structures of the measured element is yielded. Thus, in case the catalytically-active site relates to a minority of all species within the sample, it is difficult to extract the exact structure of the site. However, because X-ray absorption and emission
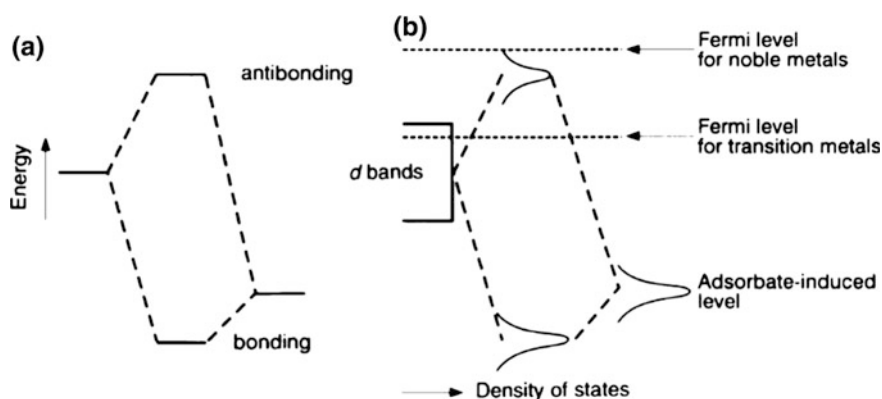
Fig. 4.2 Formation of bonding and anti-bonding states upon bonding of an adsorbate **a** with an atom and **b** on a metal surface. XAS probes the empty (anti-bonding) states and XES the filled (bonding and non-bonding) states. Reproduced with permission from [50]

spectroscopy is particularly sensitive to differences between spectra, modulation of conditions and analyzing the changes in the spectra yields the structure of the sites that respond to the modulation in the conditions [11–13]. Transient and modulation-excited spectroscopy coupled with time-resolved measuring enables the selective removal of the spectator species signals [14]. Thus an enormous enhancement of sensitivity is obtained.

During a catalytic cycle, the structure of a catalyst changes. After reactant adsorption, a chemisorbed intermediate forms, which causes a change in structure and possibly oxidation state of some of the atoms making up the catalytically-active site; Then, the surface reaction occurs, which changes the adsorbed intermediate and with that possibly the site structure; Finally desorption of the product yields the original site free of adsorbates. During a steady-state experiment, the time-averaged structure of the site will be probed, which is dominated by the resting state of the catalyst. To enable following the evolution of catalyst structure, time-resolved measurements are essential as will be highlighted in this chapter.

This chapter features selected in situ and *operando* XAS and XES experiments that relate to carbon monoxide oxidation over platinum catalysts. It is highlighted how catalyst structure and structural changes can be deduced from static and transient experimental spectra. The vast majority of atoms within a catalyst do not contribute to catalytically-active sites.

4.2 Transient X-ray Absorption Spectroscopy

Time-resolved measurements are crucial for in situ studies of dynamic chemical systems in non-steady state environments, such as the elucidation of the structure of intermediates involved in chemical processes or the kinetics of transient phenomena in the structure of the catalyst and the catalyst-reactant interface. Traditionally, the collection of XAS spectra has been slow (10–15 min per scan) so that only structural information of the progress of slow reactions could be obtained. With the advent of highly brilliant third generation synchrotron sources and the development of dedicated monochromators, detectors and data acquisition systems, structural changes that occur during reactions proceeding on timescales of (sub) seconds to several minutes can be followed. Time resolved XAS (quick XAS [15, 16] and energy dispersive XAS [17, 18]), with an ultimate time resolution of a few milliseconds per spectrum, allow to identify the structure of intermediates in catalytic reactions. When coupled with techniques to determine the performance/activity of the catalyst, for example mass spectrometry or gas chromatography, true structure-performance relationships can be obtained. However, as pointed out by Bravo-Suárez et al. [19], the sole identification of the presence of intermediate species is not sufficient proof that they are truly reaction intermediates; They could be spectator species during the actual reaction. Oyama and coworkers showed the value of transient XAS for the identification of active sites by studying the epoxidation of propylene by gold catalysts: They showed that the rate of structural

change of the titanium site corresponds to the observed global reaction rate [19]. This was one of the first reports that showed the strength of transient XAS, in which solid-state kinetic estimations were carried out by XAS spectroscopy and were directly coupled to the global reaction rate to determine if intermediates were involved in the reaction.

Gas phase reactions in an in situ catalytic cell are typically triggered by a fast exchange of reactive gases. By using gas lines and capillaries with small inner diameters and by positioning the capillaries close to the fast switching valves, reactions at the beginning of the reactor bed can be triggered within a few milliseconds. The changes then typically happen within a few tens of milliseconds up to a few seconds. Thus, in order to detect changes well, the detection limit for spectroscopy ultimately needs to be a few milliseconds. Currently there are two fundamental different approaches that reach this time resolution, each with its advantages and disadvantages. Both these techniques need very powerful X-ray sources, so-called third generation synchrotron sources, which provide at least 10^{12} monochromatic photons per second.

With QuickXAS, the monochromatic beam is selected from the polychromatic synchrotron beam by the use of a channel-cut crystal (i.e. two well defined crystal surfaces carved out in one crystal block). The first crystal selects out the energy from the polychromatic beam according to Bragg's law. The second crystal is needed to maintain a fixed exit of the beam and thus a stable beam position at the sample. This channel-cut crystal is then oscillated back and forth, i.e. moved through an energy range of a few 100 eV up to a few keV. Currently, mechanics allow for an oscillation of 50 Hz, the limitation is rather the speed of the detection system. A time resolution is achieved on the order of 10 ms for a full EXAFS spectrum (1000 eV), which is what one ultimately needs to follow solid-gas interface reactions in a capillary reactor. The main advantage of QEXAFS is that it is easily integrated into any existing XAS beamline.

The energy-dispersive XAFS technique has preceded the developments of QEXAFS and has meanwhile matured at a few synchrotron sources. Nowadays one obtains a milli-second time resolution with this technique. In energy dispersive XAS a curved crystal polychromator disperses and focuses a polychromatic X-ray beam onto the sample. The transmitted beam is then detected by a position-sensitive detector. The ultimate time resolution is only determined by the readout speed of the detector and the number of photons available in such a small time scale. EDXAS requires a very stable beamline setup and is thus available on a few dedicated beamlines.

The high time-resolution of XAS combined with modulated excitation offers the possibility to pick up small structural changes in a catalyst mediated through the modulation excitation. In a modulated excitation experiment, a material is excited with a periodically alternating external stimulation such as temperature, pressure, magnetic field, pH, potential, or concentration. At the same time the response of the catalyst is monitored with time-resolved spectroscopy. One can then analyze the large time-resolved data set either with multivariant analysis tools or with phase-sensitive detection. In phase-sensitive detection (PSD), the measured system response towards the modulated excitation, in our case the set of XAS spectra, is

filtered with the excitation frequency. Processes with periodically repeated oxidative regeneration are prime examples of such a modulation experiment, where the material is periodically exposed to alternating gas compositions. Mathematically phase-sensitive detection is described by the following equation [20]:

$$A_k^{\phi_k^{PSD}}(E) = \frac{2}{T} \int_0^T A(E,t) \sin(k\omega t + \phi_k^{PSD}) dt \qquad (4.1)$$

where $A(E, t)$ is the original signal (i.e. the XAS spectrum) as a function of time t and energy E, $k = 1$ is the fundamental harmonic, ω is the frequency of the external stimulation, ϕ_k^{PSD} is the demodulation phase angle, and $T = 1/\omega$ is the modulation period. Recent modulated excitation XAS experiments showed the feasibility of recording demodulated XAS spectra [11, 21, 22]. These studies demonstrated that minority species can be detected in modulation excitation XAS and that noise and spectator species are removed from the demodulated XAS spectra. By calculating the demodulated spectrum $A(E)$ for phase angles between 0 and 360°, the spectra are transformed from the time-domain into a phase-domain. This mathematical procedure cancels out all parts of the measured spectra that do not follow the excitation frequency ω. These parts include the spectator species and noise. Thus, demodulated spectra contain only the differences between different phase angles of the modulation period. In other words, PSD is sensitive only to the changes imposed by the external stimulus. When the XAS spectra only show two distinct states, the demodulated spectra will show the same spectral features as the difference spectrum of spectra of these two distinct states, only with much less noise [12]. The modulated excitation approach has further been applied to infrared spectroscopy [20, 23, 24], Raman spectroscopy, and to X-ray diffraction (XRD) where a correlated temporal analysis of the Raman and the XRD signals allowed a more detailed study of phase transitions [25, 26].

An alternative to phase sensitive detection to analyze the modulation-excitation XAS data set, to find the structure of a minority (active) species, is to use multivariate analysis software. This was applied recently to time-resolved XAS spectra and has great potential for determining the structure of either short-lived intermediates or of minority species [27, 28]. This approach has as additional benefit that the time evolution of the different species present is preserved.

4.3 X-ray Emission Spectroscopy

X-ray emission spectroscopy (XES) is complementary to XAS as it probes the occupied density of states around the atom of interest. XES includes a range of hard-X-ray (>5 keV) photon-in-photon-out techniques, including the analysis of the fine structure of the X-ray emission lines and resonant inelastic X-ray scattering (RIXS) [29, 30]. In comparison to conventional X-ray absorption techniques, RIXS provides an enhanced sensitivity to the electronic structure where both the occupied

and unoccupied electronic states are simultaneously probed. In a RIXS experiment the incoming photon (photon-in) excites an inner-shell electron just above the Fermi level. By tuning the incident beam energy, different unoccupied states can be probed. The remaining core-hole is filled within a few femtoseconds [31] by electronic transitions from higher shells of the atom. This electronic transition is accompanied by X-ray emission (photon-out), the energy of which depends on the electronic states involved in the decay transition and thus provides information on the occupied electronic states.

RIXS spectroscopy can be employed for the detection of electronic transitions involving core (core-to-core RIXS) or valence electrons (valence-to-core RIXS). In case of core-to-core RIXS, the initial and final electronic states of an atom are in most cases screened and therefore are rather insensitive to its chemical surrounding. For this reason, the experimental results of core-to-core RIXS can be evaluated straightforward by theoretical calculations that are based on the single-electron approximation (using for example the FEFF code [32, 33]). Moreover, these transitions provide highest X-ray rates (i.e. detected intensities) and therefore are commonly used for the detection of elements present at low concentrations.

In valence-to-core RIXS, the inner core-hole is filled by an outer-shell electron. Because of electron-electron interaction between the excited core-electron and the decaying valence-electron, detailed information about the electronic states of an atom can be obtained. In valence-to-core RIXS spectroscopy, both the incoming and outgoing photon energies are in the keV range while the probed unoccupied and occupied electronic states are only in a range of a few eV around the Fermi level. Therefore, a picture of the electronic states of the studied system can be retrieved under in situ conditions, which is challenging for electron-based techniques such as X-ray photoelectron spectroscopy (XPS). The transition rates for valence-to-core RIXS are weaker as compared to core-to-core RIXS, therefore the experiments are time consuming and usually performed on concentrated samples.

In Fig. 4.3 an exemplary $L\alpha_1$-RIXS plane of Au_2O_3 is shown that was collected at room temperature around the Au L_3 edge by detecting the $L\alpha_1$ X-ray emission resulting from the $3d_{5/2} \rightarrow 2p_{3/2}$ core-to-core transition. At an incident energy of 11920.5 eV and emission energy of 9713.5 eV a strong $2p_{3/2} \rightarrow 5d$ resonance is detected. In Fig. 4.3 (right panel), two XAS spectra extracted from the RIXS plane are plotted. By integrating the full X-ray emission intensity at each incident energy, the total fluorescence yield (TFY) spectrum was constructed, while high resolution XAS (HR-XAS) is obtained from the maximum of the $L\alpha_1$ peak intensity. The HR-XAS exhibits more pronounced features, and therefore detailed information about the 5d electronic structure can be obtained [34].

The main advantage of RIXS is that it provides a full electronic picture of the metal site of interest, under in situ conditions. Similar high-resolution XAS spectra as extracted from the RIXS planes in Fig. 4.3 can also be collected by tuning a spectrometer to the top of the emission line and varying the incident energy. Such spectra are called high-energy-resolution fluorescence-detected XAS (HERFD XAS) spectra. They have better energy resolution than regular XAS spectra and thus reflect the density of states (DOS) in more detail. This has been used for
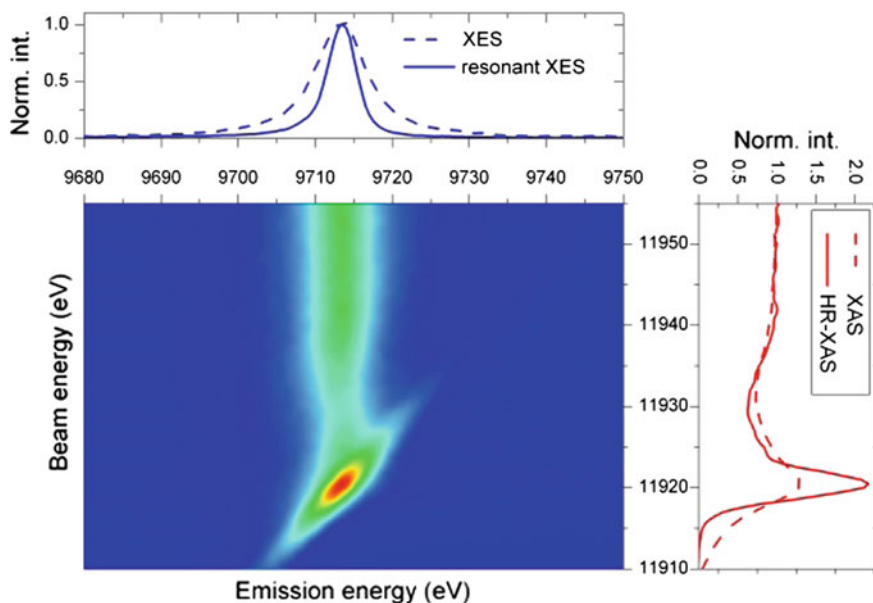
Fig. 4.3 Lα_1-RIXS plane of Au$_2$O$_3$ around the Au L$_3$ absorption edge. *Right* the TFY and HR-XAS spectra. *Top* resonant and non-resonant XES spectra. Reproduced with permission from [52]

example to explore the Cu K-edge XANES region of copper-loaded zeolites under in situ conditions [35, 36] (Fig. 4.4) to follow the changes in the copper sites of Cu-MOR (a medium pore-size zeolite) during different stages of partial oxidation of methane. The features in the pre-edge region of the spectra can be explained by the contribution of two oxidation states. Other features result from shake-up and shake-down processes which depend on the ligand and on the structure of the copper centers in the zeolite [36]. These studies of the unoccupied DOS provide useful insight in the reaction mechanism and the number of copper sites involved in the reaction, which turned out to be significantly larger than previously thought based on extraction studies [36].

The Kβ main line spectra are dominated by the valence shell spin state contributions and thus enable the detection of oxidation state changes and high-spin low-spin transitions. The spin sensitivity arises from an intra-atomic interaction between the 3p and 3d shells [6]. The satellite lines, i.e. the emission lines just below the Fermi level or alternatively the valence-to-core transitions (denoted Kβ'' or K$\beta_{2,5}$), show great sensitivity to changes in the chemical environment, such as ligand identity, ligand ionization state, and hybridization state [37]. The formal electronic configuration in the final state of the X-ray emission transition is identical to valence electron photoemission, such as X-ray photoelectron spectroscopy. However, there are some important differences between XPS and XES [38]. XES is a strictly element-specific probe; Only the electron density of the absorbing atom
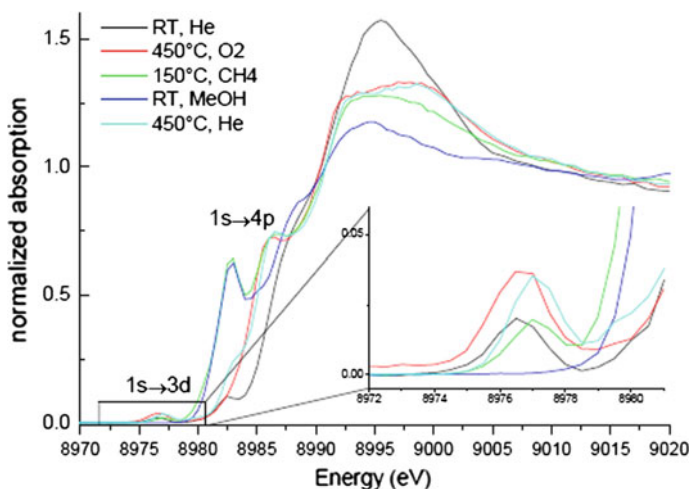
Fig. 4.4 Cu K edge HERFD XAS spectra of Cu-zeolites under different gas atmospheres show rich pre-edge features. Copper reduces from Cu^{2+} to a mixture of Cu^+ and Cu^{2+} states upon interaction with methane. Shake-up and shake-down processes are also present in the pre-edge region [36]. Reproduced with permission from [36]

and its direct environment is probed with a considerably simpler analysis than for XPS experiments. The selection rules for electron transitions in K-edge XES only allow for orbitals to be detected that have p-contribution with respect to the metal atom. Furthermore, XES probes the bulk and not only the surface of the sample and vacuum conditions are not required.

Valence-to-core RIXS spectroscopy enables to probe the electronic structure of the shared electrons of the ligand environment of a metal of interest [37, 39, 40]. Since this is a very 'photon-hungry' technique, time-resolved experiments are limited, and only a static picture of the electronic state can be obtained. As an example, the unoccupied electronic states of titania (anatase) were probed by exciting the 1s electron above the Fermi level and probing the occupied electronic states by detecting the following 3p → 1s and valence → 1s decay transitions [41]. The recorded RIXS plane of titania is plotted in Fig. 4.5. The RIXS plane consists of well-separated pre-edge structures at beam energies between 4968 and 4975 eV and post-edge features at higher excitation energies.

Based on the HR-XAS and non-resonant XES spectra, the valence and conduction band electronic states can be extracted from the measured RIXS plane. The curves were scaled to the Fermi energy by shifting the energy axis of each spectrum by a value of 4965.4 eV. This energy was extracted from the inflection point of the valence-to-core transition (dashed line in Fig. 4.6). Figure 4.6 plots the recalibrated and renormalized spectra, which are compared to the density of states calculated with the FEFF8.4 code [33]. The titanium and oxygen DOS for Ti are plotted in Fig. 4.6 (bottom). The DOS computation shows that the pre-edge structure mainly consists of Ti d-states and the contribution of the oxygen p-states is negligibly
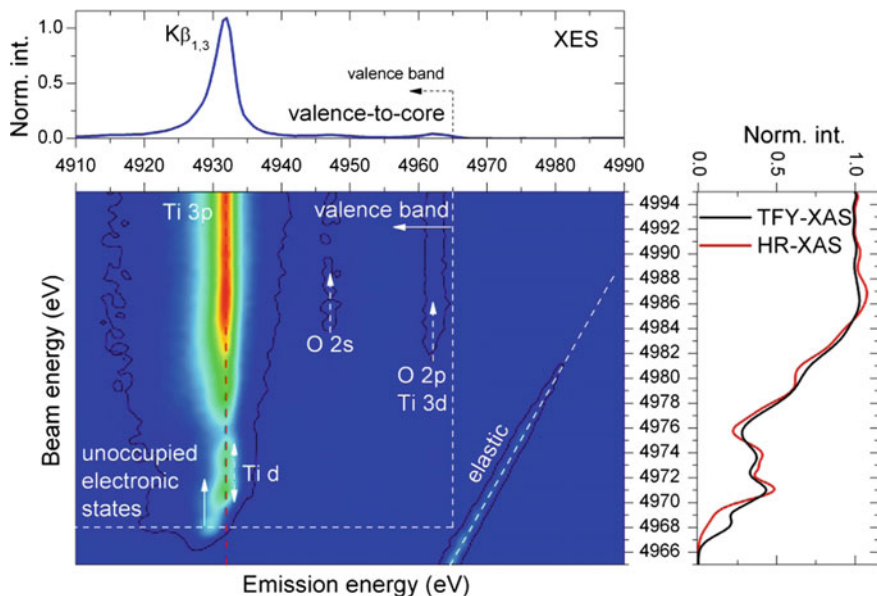
Fig. 4.5 The $K_{1,3}$ and valence-to-core RIXS for anatase. The electronic bands contributions are schematically marked in the figure. *Top* XES spectrum for incident X-ray energies tuned above the absorption edge. *Right* comparison of high-resolution XAS and total-fluorescence XAS spectra. Reproduced with permission from [41]

Fig. 4.6 (*Top*) Occupied (*blue*) and unoccupied (*red*) electronic states of titania extracted from the RIXS plane. The measured data are compared to DOS calculations (*bottom*) [41]. Reproduced with permission from [41]
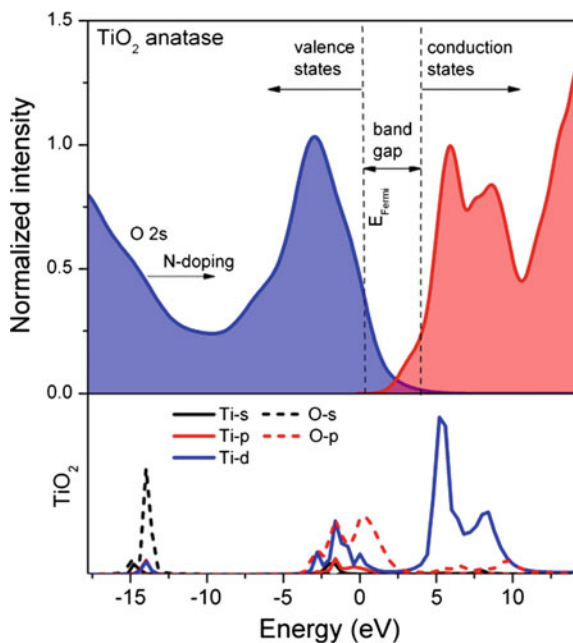
small. For the occupied electronic states just below the Fermi level an equal contribution of O-p and Ti-d orbitals is observed. An additional weak structure can be seen at around -15 eV that results from the 2s orbital of oxygen [41].

4.4 Examples

4.4.1 Carbon Monoxide Oxidation: Time-Resolved X-ray Absorption

The electronic structure of metal nanoparticles is strongly dependent on the presence and nature of adsorbates, and these adsorbates in turn affect the shape and intensity of features in the XAS spectrum. This makes XAS an attractive tool for investigating reactions like carbon monoxide oxidation, where multiple potential adsorbates are present and the catalyst structure depends on the reaction conditions. An early study showing the potential of the technique for investigating the adsorption of reactant molecules on a platinum catalyst was published by Safonova et al. in 2006 [7]. While this work did not constitute an *operando* experiment, it demonstrated the observation of differences in the electronic structure of platinum nanoparticles under realistic conditions. A particular emphasis was put on the comparison between conventional and HERFD XAS. While the former is able to distinguish between surface-oxidized, carbon-monoxide-covered, and bare platinum, the improved energy resolution of HERFD XAS gives additional electronic information. This information could be combined with theoretical calculations to show that atop adsorption of carbon monoxide is the dominant conformation under the measured conditions.

Based on this demonstration of the potential of XAS and HERFD XAS for studying platinum structure under reaction conditions, Singh et al. combined both techniques to investigate structural changes in platinum during light-off under realistic reaction conditions and with simultaneous monitoring of conversion [42]. The combination of both techniques is desirable, since the high time resolution of QEXAFS permits following the structural changes during light-off (Fig. 4.7), whereas the better energy resolution of HERFD XAS gives a more detailed picture of the initial and final states of the catalyst.

High-energy resolution off-resonant X-ray spectroscopy (HEROS) combines the attractive features of HERFD XAS and QEXAFS by enabling the recording of spectra with high time- and energy resolution. This was demonstrated by Szlachetko et al. for cyclic switching between oxygen and carbon monoxide over a platinum-based catalyst [43]. While the cyclical operation required for HEROS is distinct from the way most catalytic reactors are operated, the method gives fundamental insights into the steps required in the catalytic reaction under realistic conditions.

Oscillating reactions in carbon monoxide oxidation have also received considerable attention in XAS studies. The main motivation of such work was finding correlations between changes in structure and oxidation state of the metal in the

Fig. 4.7 XANES spectra (**a**) and carbon monoxide conversion (**b**) during heating-induced light-off in carbon monoxide oxidation over platinum. The Pt L_3 edge XANES spectra reveal that the transition from carbon-monoxide-covered platinum to oxidized platinum coincides with a sudden increase in activity
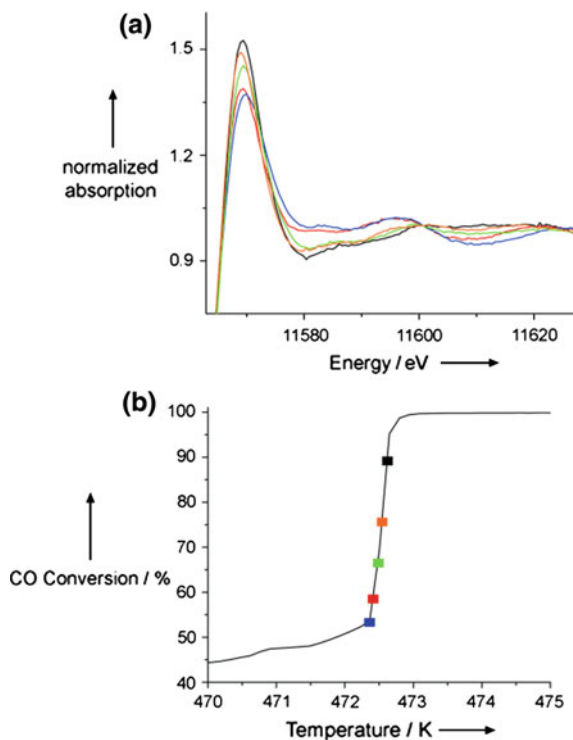
catalyst, and the oscillating conversion. Singh et al. used a combination of mass spectrometry, quick XAS and infrared spectroscopy to follow adsorbate concentrations, platinum oxidation state, and conversion during cooling, which includes significant oscillatory phenomena [44]. XANES was measured in multiple positions along the direction of flow, and it was found that further downstream in the reactor the catalyst reduced at lower conversion levels, i.e. that the reduction proceeded from the inlet side in a downstream direction.

Boubnov et al. used a combination of XAS and DRIFTS to investigate oscillatory phenomena in carbon monoxide oxidation during heating [45]. Comparing the changes in whiteline intensity with temperature at different positions, they observed that oscillations start at lower temperatures closer to the outlet side of the reactor. While this result may appear to contradict the results of Singh et al., it must be noted that one experiment was carried out while heating, and the other while cooling. Both experiments were carried out in excess oxygen, resulting in an increase of the oxygen/carbon monoxide ratio throughout the reactor during catalytic conversion. It is therefore expected that the reduction of the platinum during cooling initiates where conditions are most reducing (i.e. near the inlet), whereas oxidation during heating initiates where they are most oxidizing (i.e. near the outlet).

Figueroa and Newton used energy dispersive XAS and DRIFTS to investigate oscillatory behavior in carbon monoxide oxidation on a rhodium catalyst [46].

Unlike the examples discussed for platinum, the oscillations over the rhodium catalyst did not appear to be driven by changes in the oxidation state of the metal. Instead, they suggest a mechanism based on the presence of atomic carbon on the sample, which does not result in changes detectable by XAS.

4.4.2 Adsorption of Carbon Monoxide: High Energy Resolution XAS Spectra

Reactant adsorption is an essential step in every catalytic reaction, irrespective of the reaction mechanism. Carbon monoxide oxidation is generally assumed to occur by a Langmuir-Hinshelwood-type mechanism, in which both oxygen and carbon monoxide are chemisorbed on the surface and react with each other [47]. Carbon monoxide poisoning of a noble metal catalyst is often observed where the surface is covered by carbon monoxide. Desorption is needed to free a site for oxygen to react [48]. X-ray based methods provide fundamental insight into the bonding of carbon monoxide on nano-sized particles [49]. X-ray absorption spectra provide the element- and spin-selective density of states. The Pt L_3 edge probes the empty d density of states directly above the Fermi level and thus probes empty non-bonding and anti-bonding states. A disadvantage of adsorption edges of such high energy is that the spectra are broad and spectral detail may be lost. High energy resolution fluorescence detected (HERFD) XAS yields spectra of high energy resolution, which highlight many more spectral details. Such an experiment was pioneered on platinum by Sofanova et al., as discussed above [7]. The origin of spectral energy resolution is the lifetime of the final state; In a HERFD experiment, specific fluorescence decay channels are selectively probed. This fluorescence channel leaves a new core hole that has a lower core-hole lifetime broadening, resulting in less spectral broadening. It is essential to use a fluorescence/emission detector that has an energy resolution equal to or better than the lifetime broadening of the new final state. This results in spectra that have enhanced spectral resolution. Figure 4.8 shows typical Pt L_3 edge spectra of nano-sized platinum particles, here supported on alumina.

These spectra illustrate the empty d density of states of particles free of adsorbates, with carbon monoxide adsorbed, and after oxidation of their surface. Especially the spectrum of the particles covered in carbon monoxide is revealing. Compared to the spectrum of the particles free of adsorbates, an upwards energy shift is observed. Such shift in Fermi level identifies charge transfer from the platinum 5d orbitals to carbon monoxide. Moreover, the first intense spectral feature, the so-called whiteline, is split into a doublet, the high-energy component originating from a newly-formed anti-bonding orbital between platinum d and carbon and oxygen s and p orbitals. Carbon monoxide can adsorb on different sites on metal surfaces: on atop, bridged and threefold sites binding to respectively one, two, and three metal atoms. Because each such site has a different electronic configuration, XAS spectra are sensitive to the mode of bonding, which can be

Fig. 4.8 Pt L_3 edge **a** XAS and **b** HERFD XAS of platinum nano-particles on alumina free of adsorbates (*black*), after surface oxidation (*red*), and covered in carbon monoxide (*green*). The higher energy resolution of HERFD XAS permits the differentiation between different possible carbon monoxide adsorption sites. Reproduced with permission from [7]
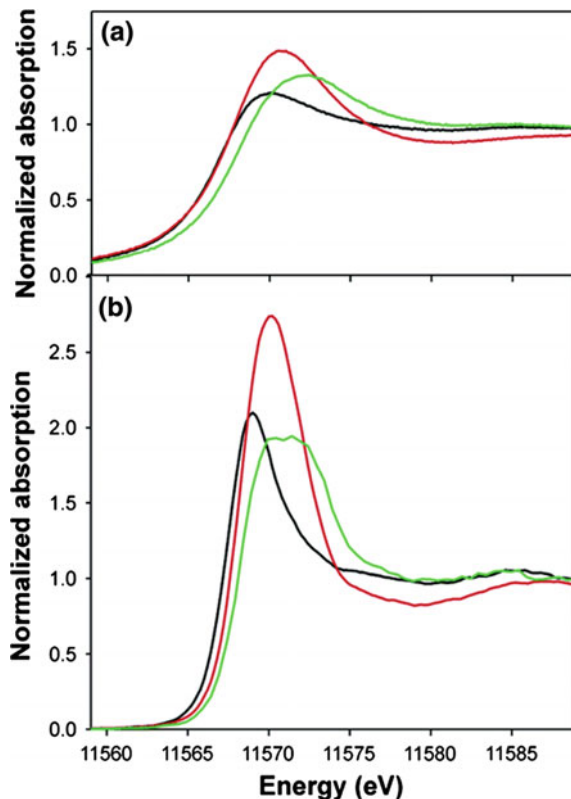
assessed by theoretical modeling relatively easily [4]. Fortuitously, the simulated Pt L_3 spectrum of atop bonded carbon monoxide deviates from other adsorption modes and can be quantitatively assessed. Theory thus unambiguously identifies the adsorption mode of carbon monoxide as bonded to a single metal atom in an atop fashion. In this case, the high energy resolution helped to unambiguously identify the adsorption site. Normal XAS showed the shift in absorption edge, however, did not resolve the doublet complicating unambiguous spectral assignment.

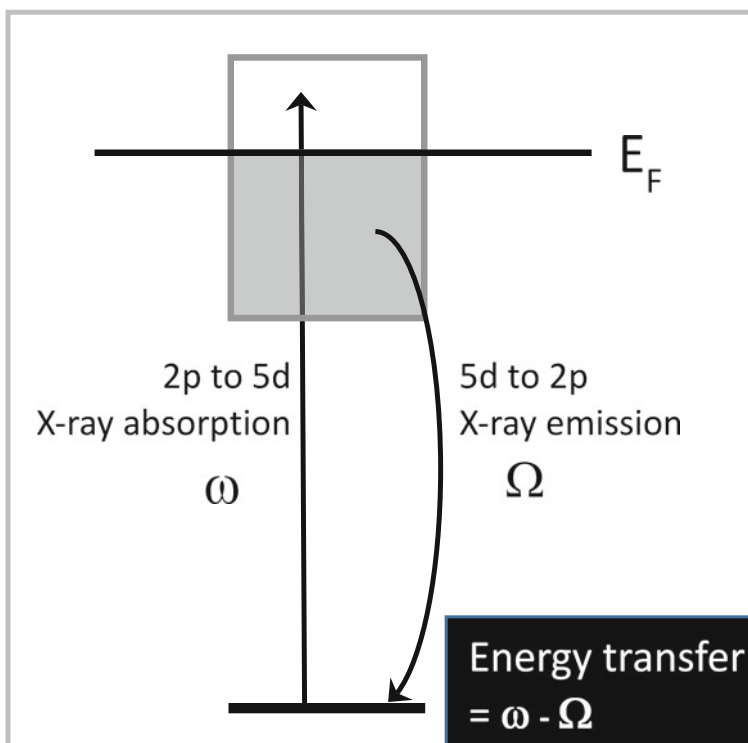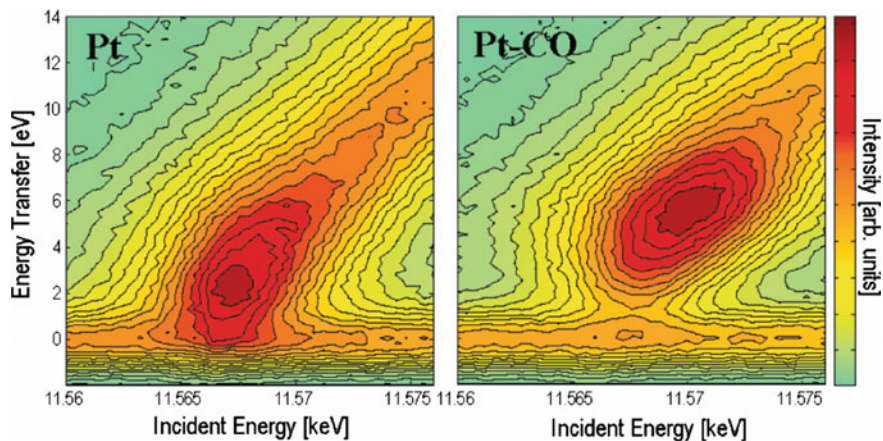### 4.4.3 Adsorption of Carbon Monoxide: Valence-to-Core RIXS

Bonding originates from forming bonding and anti-bonding states [50]. In XAS, the orbitals above the Fermi level are probed, in XES those that are filled. Thus, an experiment, which probes the valence band directly probes the bonding states. Such an experiment has been done on the same platinum nano-particles [34] as the HERFD XAS study described above. In such a valence-to-core resonance inelastic

X-ray scattering (valence-to-core RIXS) experiment, an electron from a core level is excited (X-ray absorption) and the resulting fluorescence valence-to-core decay (X-ray emission) is detected as function of energy (Fig. 4.9). The resulting plot depicts the filled 5d density of states, the Fermi energy at 0 eV. The nanoparticles free of adsorbates have the d band cut through the Fermi level, whereas after carbon monoxide adsorption, a shift of the Fermi level is observed, which is illustrative of a band gap opening. The band shift is towards positive energy transfer, thus higher binding energy. Such a shift lowers the energy levels of the bonding and anti-bonding states with adsorbates, decreasing the reactivity [34] of the platinum nanoparticles. Thus, covering platinum particles with carbon monoxide not only occupies reactive sites, but also decreases the reactivity towards other reactants, such as oxygen. Overall, carbon monoxide passivates the nanoparticles (Fig. 4.9).

4.4.4 Time-Resolved X-ray Emission: Catalytically Active and Spectator Species

Heterogeneous catalysts generally consist of multiple components; Catalytic particles are attached to a support, which are often not inert. The support affects the catalytic performance by changing the electronic and/or geometric structure of the nanoparticles and they can even catalyze one or more reaction steps. Both factors play a role in oxidation of carbon monoxide over supported catalysts. Because of the poisoning effect of carbon monoxide on the reaction, as illustrated in Fig. 4.11, a support that helps to activate oxygen enhances the rate of reaction. Thus, redox-active supports yield more active catalysts. Ceria is a well-known redox-active material and is a component in many commercial catalysts, notably in automotive exhaust. Ceria is a so-called oxygen-storage material: Release of oxygen reduces Ce^{4+} to Ce^{3+}; Oxygen uptake re-oxidizes the Ce^{3+}. The oxygen-storage capacity is defined as the amount of oxygen that can be reversibly released under defined conditions. It relates to the fraction of Ce^{3+} that can reversibly be formed. The oxygen in the support can thus be used to maintain an oxidative reaction, whenever gas-phase oxygen becomes depleted. It is generally assumed that both the oxygen-storage capacity and Ce^{3+} play essential roles in the catalytic mechanism, however, their precise contributions are debated. A recent study, employing transient conditions, identified the role of Ce^{3+} in the oxidation of carbon monoxide. The study emphasized the existence of spectator species that do not contribute to catalytic conversion [14].

Figure 4.10a shows schematically the experimental setup that was used to measure time-resolved resonance X-ray emission spectrum (RXES) of nano-sized platinum particles on ceria. The catalyst was positioned within a capillary reactor, which was connected at one side to a gas-dosing system and at the other to a mass spectrometer. The gas-dosing system allowed precise control of the gas composition, which was periodically changed from containing oxygen and carbon monoxide in a ratio of four

Fig. 4.9 (*Top*) 2p$_{3/2}$ valence-to-core RIXS of alumina-supported platinum nanoparticles before (*left*) and after (*right*) adsorption of carbon monoxide. The energy transfer is depicted as function of excitation or absorption energy. (*bottom*) Energy transition in the RIXS experiment. The incident energy excites an electron from the 2p shell into the empty 5d band; the emission from the filled 5d band into the resulting core hole is detected with high energy resolution. The relative energies are not drawn to scale. Top figure reproduced with permission from [34]
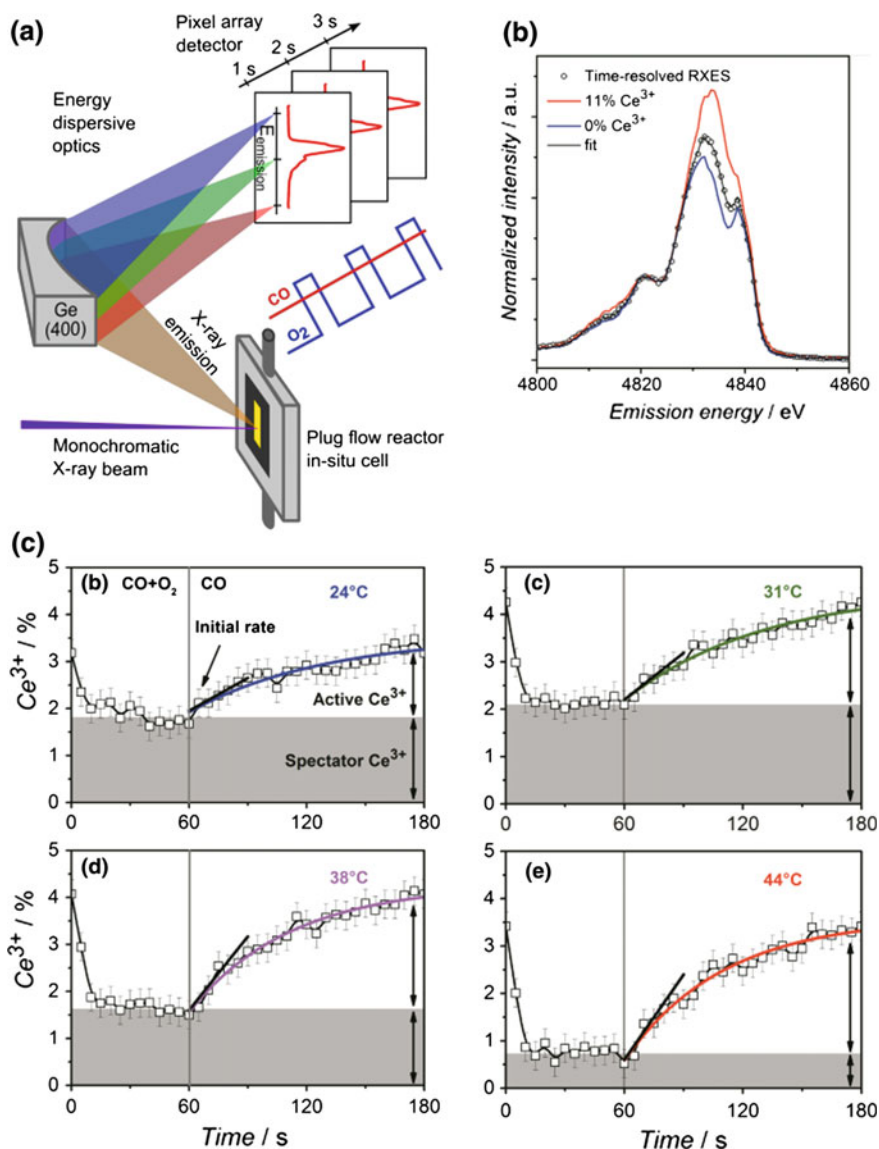
Fig. 4.10 a Setup to measure time-resolved RXES spectra in a single shot. **b** RXES spectra of materials with known amounts of Ce^{3+} and Ce^{4+} used to quantify the spectra during the transient experiment. **c** Development of the amounts of Ce^{3+} in Pt/ceria after the switch from carbon monoxide to oxygen/carbon monoxide at four different temperatures. Reproduced with permission from [14]

to one to containing only carbon monoxide. The conditions were chosen such that the maximum conversion always remained below 10% to ensure differential conditions. The rate of structural change of cerium was followed by time-resolved RXES.
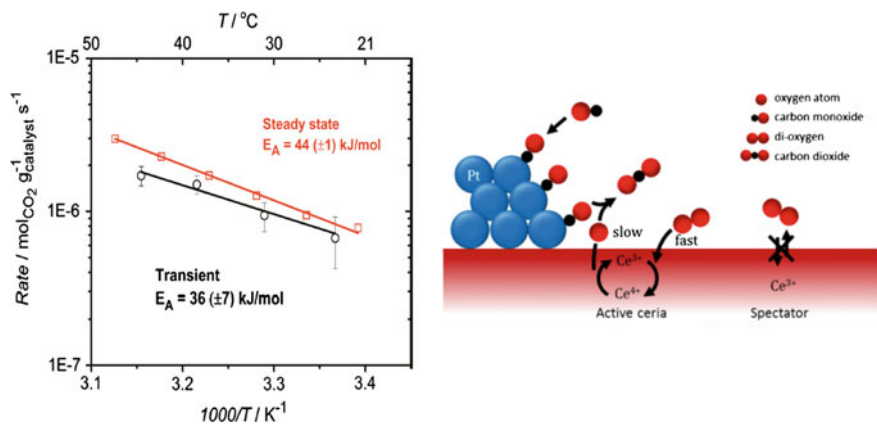
Fig. 4.11 (*Left*) Arrhenius plot of rate of steady-state carbon monoxide oxidation (*red*) and of initial rate of Ce^{4+} reduction after the switch from catalytic conditions to carbon monoxide. (*Right*) Possible reaction mechanism over ceria supported platinum. The platinum nanoparticles capture carbon monoxide, which reacts at the metal-support interface with an oxygen atom from the support, thereby reducing Ce^{4+} to Ce^{3+}. If oxygen is present in the gas phase, Ce^{3+} is very rapidly re-oxidized, making the active Ce^{3+} a short-lived reaction intermediate. Long-lived Ce^{3+} does not participate directly in the catalytic cycle. Reproduced with permission from [14]

Therefore, the catalyst was exposed to monochromatic X-rays and the $2p_{3/2}5d_{5/2}$ emission line was detected using a von Hamos-type spectrometer [51]. Such detector enables recording the complete emission spectrum in a single shot (Fig. 4.10a). Such arrangement of excitation and detection enables reaching high time resolutions, fundamentally limited by the readout time of the detector and the signal-to-noise ratio. Continuous measuring during multiple switches increases the signal-to-noise ratio. Because the $2p_{3/2}5d_{5/2}$ emission line is sensitive to the cerium oxidation state (Fig. 4.10b), the experiment allows determining the rates of Ce^{3+} formation and disappearance directly after the switches in gas composition (Fig. 4.10c). The experiment performed at 24 °C (top left in c) illustrates that, under catalytic conditions, slightly less than 2% of all cerium is Ce^{3+}. This amount decreases with increasing temperature to less than 1% at 44 °C. At all temperatures, there is an increase in the fraction of Ce^{3+} directly after the switch to an atmosphere only containing carbon monoxide. The initial rate of Ce^{3+} formation, indicated by the straight lines, increases with temperature enabling plotting an Arrhenius plot. This plot, after correction for stoichiometry, is compared to the rate of carbon monoxide oxidation under steady state conditions (Fig. 4.11 left), which was measured under identical conditions in the same reactor using gas chromatography. The lines measured by RXES and kinetic measurements coincide and are within the accuracy of measurements the same. This illustrates that directly after the switch, the reaction continues with exactly the same rate and that the oxygen atom originates from ceria. The consequence is that reduction of ceria is coupled to the rate-limiting step. Re-oxidation that occurred after the switch back to carbon monoxide and oxygen was very rapid and

too fast to determine its kinetics. Thus, under steady-state catalytic conditions, the catalytically active cerium is virtually completely Ce^{4+}, and Ce^{3+} is a short-lived reaction intermediate (Fig. 4.11 right). Any Ce^{3+} that is present under steady-state conditions, is a spectator species and does not directly play a role in the reaction mechanism.

4.5 Conclusions

XAS and XES are excellent methods to identify the structure of catalysts under reaction conditions and within an actual reactor. They enable to determine the local geometric and electronic structure of a catalyst element specifically and with high time- and space resolution. Because the structure of platinum catalysts for the oxidation of carbon monoxide varies strongly with conditions, structural changes within a single reactor may occur. The different phases have different activity and, therefore, the precise relationship between structure of active sites and activity has in most cases not been established. The structure of the phase that is responsible for activity and that of the active site that performs the catalytic turnover must be distinguished.

Transient, modulated, and space-resolved experiments have established the structure of the phase that is associated with the low-activity phase; The platinum surface is maximally covered with carbon monoxide and oxygen activation over the metal only occurs after partial carbon monoxide desorption, which frees sites for oxygen activation. Much higher rates occur in case oxygen is activated on the support, such as ceria. Reaction than occurs at the metal—support interface.

The structure of platinum in the highly active state is much less established. It is associated with oxygen at the surface. The catalyst activity has been shown to scale with the presence of a platinum surface oxide, however, also reduced states are suggested. The exact structure of the surface oxide is not established, other than that it is disordered and defective. It can be speculated that such sites are responsible for binding carbon monoxide and that oxygen atoms in its vicinity react to form carbon dioxide.

It is safe to say that the site on a platinum catalyst that is responsible for oxygen activation and its subsequent reaction to carbon monoxide has not been unambiguously established. It is very well possible that within a single reactor, multiple structures are responsible for oxygen activation. Part of the origin of the absence of agreement originates from often strongly varying conditions, which affect catalyst structure and thus influence the outcome of the experiment. A complete description of active sites can only be achieved after quantitative determination of local gas composition and catalyst structure throughout the whole catalytic reactor. Combining such an experiment with complementary methods, such as vibrational spectroscopy enhances the chances of success.

References

1. S. Bordiga et al., Reactivity of surface species in heterogeneous catalysts probed by in situ X-ray absorption techniques. Chem. Rev. **113**(3), 1736–1850 (2013)
2. C. Lamberti et al., XAS Spectroscopy: related techniques and combination with other spectroscopic and scattering methods, in X-Ray Absorption and X-Ray Emission Spectroscopy: Theory and Applications, ed. by J.A. van Bokhoven, C. Lamberti (Wiley, Chichester (UK), 2016), pp. 303–350
3. P.M. Abdala et al., Scientific opportunities for heterogeneous catalysis research at the SuperXAS and SNBL beam lines. CHIMIA Int. J. Chem. **66**(9), 699–705 (2012)
4. D.E. Ramaker, D.C. Koningsberger, The atomic AXAFS and [capital Delta][small mu] XANES techniques as applied to heterogeneous catalysis and electrocatalysis. Phys. Chem. Chem. Phys. **12**(21), 5514–5534 (2010)
5. D.C. Koningsberger et al., XAFS spectroscopy; fundamental principles and data analysis. Top. Catal. **10**(3–4), 143–155 (2000)
6. P. Glatzel, U. Bergmann, High resolution 1s core hole X-ray spectroscopy in 3d transition metal complexes—electronic and structural information. Coord. Chem. Rev. **249**(1–2), 65–95 (2005)
7. O.V. Safonova et al., Identification of CO adsorption sites in supported Pt catalysts using high-energy-resolution fluorescence detection X-ray spectroscopy. J. Phys. Chem. B **110**(33), 16162–16164 (2006)
8. J. Singh, C. Lamberti, J.A. van Bokhoven, Advanced X-ray absorption and emission spectroscopy: in situ catalytic studies. Chem. Soc. Rev. **39**(12), 4754–4766 (2010)
9. F. Bonino et al., Catalyst characterization by Xas And Xes spectroscopies: in situ and operando experiments, in Synchrotron Radiation, ed. by S. Mobilio, F. Boscherini, C. Meneghini (Springer, Berlin, 2015), pp. 717–736
10. M. Dreher et al., Design of a continuous-flow reactor for in situ x-ray absorption spectroscopy of solids in supercritical fluids. Rev. Sci. Instr. **83**(5), 054101 (2012)
11. D. Ferri, M.A. Newton, M. Nachtegaal, Modulation excitation X-ray absorption spectroscopy to probe surface species on heterogeneous catalysts. Top. Catal. **54**(16), 1070–1078 (2011)
12. C.F.J. König et al., Quantitative analysis of modulated excitation X-ray absorption spectra: enhanced precision of EXAFS fitting. J. Phys. Chem. C **116**(37), 19857–19866 (2012)
13. D. Ferri et al., Synchrotron high energy X-ray methods coupled to phase sensitive analysis to characterize aging of solid catalysts with enhanced sensitivity. Phys. Chem. Chem. Phys. **15**(22), 8629–8639 (2013)
14. R. Kopelent et al., Catalytically active and spectator Ce^{3+} in ceria-supported metal catalysts. Angew. Chem. Int. Ed. **54**(30), 8728–8731 (2015)
15. R. Frahm, J. Stötzel, D. Lützenkirchen-Hecht, advancing time-resolved methods in monitoring and characterization of catalysts. Synchrotron Radiat. News **22**(2), 6–11 (2009)
16. M. Nachtegaal et al., QEXAFS: techniques and scientific applications for time-resolved XAS, in X-Ray Absorption and X-Ray Emission Spectroscopy: Theory and Applications, ed. by J.A. van Bokhoven, C. Lamberti (Wiley, Chichester (UK), 2016), pp. 155–183
17. M.A. Newton, A.J. Dent, J. Evans, Bringing time resolution to EXAFS: recent developments and application to chemical systems. Chem. Soc. Rev. **31**(2), 83–95 (2002)
18. O. Mathon, I. Kantor, S. Pascarelli, Time-resolved XAS using an energy dispersive spectrometer: techniques and applications, in X-Ray Absorption and X-Ray Emission Spectroscopy: Theory and Applications, ed. by J.A. van Bokhoven, C. Lamberti (Wiley, Chichester (UK), 2016), pp. 185–212
19. J.J. Bravo-Suárez et al., Transient technique for identification of true reaction intermediates: hydroperoxide species in propylene epoxidation on gold/titanosilicate catalysts by X-ray absorption fine structure spectroscopy. J. Phys. Chem. C **112**(4), 1115–1123 (2008)
20. D. Baurecht, U.P. Fringeli, Quantitative modulated excitation Fourier transform infrared spectroscopy. Rev. Sci. Instr. **72**(10), 3782–3792 (2001)

21. A. Eyssler et al., Improvement of catalytic activity of LaFe0.95Pd0.05O3 for methane oxidation under transient conditions. J. Phys. Chem. C **115**(4), 1231–1239 (2011)
22. D. Ferri et al., First steps in combining modulation excitation spectroscopy with synchronous dispersive EXAFS/DRIFTS/mass spectrometry for in situ time resolved study of heterogeneous catalysts. Phys. Chem. Chem. Phys. **12**(21), 5634–5646 (2010)
23. E.E. Ortelli, A. Wokaun, Use of periodic variations of reactant concentrations in time resolved FTIR studies of heterogeneously catalysed reactions. Vib. Spectrosc. **19**(2), 451–459 (1999)
24. T. Bürgi, A. Baiker, In situ infrared spectroscopy of catalytic solid−liquid interfaces using phase-sensitive detection: enantioselective hydrogenation of a pyrone over Pd/TiO2. J. Phys. Chem. B **106**(41), 10649–10658 (2002)
25. A. Urakawa et al., Combined, modulation enhanced X-ray powder diffraction and raman spectroscopic study of structural transitions in the spin crossover material [Fe(Htrz)2(trz)](BF4). J. Phys. Chem. C **115**(4), 1323–1329 (2011)
26. D. Chernyshov et al., Kinematic diffraction on a structure with periodically varying scattering function. Acta Crystallographica Section A **67**(4), 327–335 (2011)
27. A. Rochet et al., Influence of the preparation conditions of oxidic NiMo/Al2O3 catalysts on the sulfidation ability: a quick-XAS and raman spectroscopic study. J. Phys. Chem. C **119**(42), 23928–23942 (2015)
28. W.H. Cassinelli et al., Multivariate curve resolution analysis applied to time-resolved synchrotron X-ray absorption spectroscopy monitoring of the activation of copper alumina catalyst. Catal. Today **229**, 114–122 (2014)
29. A. Kotani, S. Shin, Resonant inelastic X-ray scattering spectra for electrons in solids. Rev. Mod. Phys. **73**(1), 203–246 (2001)
30. U. Bergmann et al., High-resolution X-ray spectroscopy of rare events: a different look at local structure and chemistry. J. Synchrotron Radiat. **8**(2), 199–203 (2001)
31. J.L. Campbell, T. Papp, Widths of the atomic K-N7 levels. At. Data Nucl. Data Tables **77**(1), 1–56 (2001)
32. J.J. Rehr et al., Parameter-free calculations of X-ray spectra with FEFF9. Phys. Chem. Chem. Phys. **12**(21), 5503–5513 (2010)
33. J.J. Rehr et al., Ab initio theory and calculations of X-ray spectra. C.R. Phys. **10**(6), 548–559 (2009)
34. P. Glatzel et al., In situ characterization of the 5d density of states of Pt nanoparticles upon adsorption of CO. J. Am. Chem. Soc. **132**(8), 2555–2557 (2010)
35. E. Kleymenov et al., Five-element Johann-type X-ray emission spectrometer with a single-photon-counting pixel detector. Rev. Sci. Instrum. **82**(6), 065107 (2011)
36. E.M. Alayon et al., Catalytic conversion of methane to methanol over Cu-mordenite. Chem. Commun. **48**(3), 404–406 (2012)
37. O.V. Safonova et al., Local environment of vanadium in V/Al/O-mixed oxide catalyst for propane ammoxidation: Characterization by in situ valence-to-core X-ray emission spectroscopy and X-ray absorption spectroscopy. J. Catal. **268**(1), 156–164 (2009)
38. G. Smolentsev et al., X-ray emission spectroscopy to study ligand valence orbitals in Mn coordination complexes. J. Am. Chem. Soc. **131**(36), 13161–13167 (2009)
39. U. Bergmann et al., Chemical dependence of interatomic X-ray transition energies and intensities—a study of Mn Kβ″ and Kβ2, 5 spectra. Chem. Phys. Lett. **302**(1–2), 119–124 (1999)
40. C.J. Pollock, S. DeBeer, Valence-to-core X-ray emission spectroscopy: a sensitive probe of the nature of a bound ligand. J. Am. Chem. Soc. **133**(14), 5594–5601 (2011)
41. J. Szlachetko, J. Sa, Rational design of oxynitride materials: from theory to experiment. CrystEngComm **15**(14), 2583–2587 (2013)
42. J. Singh et al., Generating highly active partially oxidized platinum during oxidation of carbon monoxide over Pt/Al2O3. In situ, time-resolved, and high-energy-resolution X-ray absorption spectroscopy. Angew. Chem. Int. Ed. **47**(48), 9260–9264 (2008)

43. J. Szlachetko et al., Subsecond and in situ chemical speciation of Pt/Al2O3 during oxidation-reduction cycles monitored by high-energy resolution off-resonant X-ray spectroscopy. J. Am. Chem. Soc. **135**(51), 19071–19074 (2013)
44. J. Singh et al., Dynamic structure changes of a heterogeneous catalyst within a reactor: oscillations in CO oxidation over a supported platinum catalyst. Chemcatchem **2**(6), 653–657 (2010)
45. A. Boubnov et al., Oscillatory CO oxidation over Pt/Al2O3 catalysts studied by in situ XAS and drifts. Top. Catal. **56**(1–8), 333–338 (2013)
46. S.J.A. Figueroa, M.A. Newton, What drives spontaneous oscillations during CO oxidation using O2 over supported Rh/Al2O3 catalysts? J. Catal. **312**, 69–77 (2014)
47. M. Chen, Y. Zheng, H. Wan, Kinetics and active surfaces for CO oxidation on Pt-group metals under oxygen rich conditions. Top. Catal. **56**(15–17), 1299–1313 (2013)
48. X. Su et al., High-pressure CO oxidation on Pt(111) monitored with infrared—visible sum frequency generation (SFG). J. Am. Chem. Soc. **119**(17), 3994–4000 (1997)
49. N. Guo et al., Determination of CO, H2O and H2 coverage by XANES and EXAFS on Pt and Au during water gas shift reaction. Phys. Chem. Chem. Phys. **12**(21), 5678–5693 (2010)
50. B. Hammer, J.K. Norskov, Why gold is the noblest of all the metals. Nature **376**(6537), 238–240 (1995)
51. J. Szlachetko et al., A von Hamos x-ray spectrometer based on a segmented-type diffraction crystal for single-shot x-ray emission spectroscopy and time-resolved resonant inelastic x-ray scattering studies. Rev. Sci. Instr. **83**(10), 103105 (2012)
52. J. Szlachetko et al., In situ hard X-ray quick RIXS to probe dynamic changes in the electronic structure of functional materials. J. Electron Spectrosc. Relat. Phenom. **188**, 161–165 (2013)